Haverford College
Haverford Scholarship

Faculty Publications | Physics

1993

HCO+, H13CN, and H12CN Aperture Synthesis Observations of the Circumnuclear Molecular Ring in the Galactic Center

Jonathan M. Marr
Haverford College, jmarr@haverford.edu

Follow this and additional works at: https://scholarship.haverford.edu/physics_facpubs

Repository Citation

"HCO+, H13CN, and H12CN Aperture Synthesis Observations of the Circumnuclear Molecular Ring in the Galactic Center" by J. M. Marr, M. C. H. Wright, and D. C. Backer 1993, Astrophys. J., 411, 667

This Journal Article is brought to you for free and open access by the Physics at Haverford Scholarship. It has been accepted for inclusion in Faculty Publications by an authorized administrator of Haverford Scholarship. For more information, please contact nmedeiro@haverford.edu.

1993ApJ...411..667M

THE ASTROPHYSICAL JOURNAL, 411:667–673, 1993 July 10
© 1993. The American Astronomical Society. All rights reserved. Printed in U.S.A.

HCO^+, $H^{13}CN$, AND $H^{12}CN$ APERTURE SYNTHESIS OBSERVATIONS OF THE CIRCUMNUCLEAR MOLECULAR RING IN THE GALACTIC CENTER

J. M. MARR,[1] M. C. H. WRIGHT,[2] AND D. C. BACKER[2]
Received 1992 November 5; accepted 1993 January 12

ABSTRACT

We observed Sgr A West in the $J = 1 \rightarrow 0$ transition lines of $H^{13}CN$ and HCO^+ with a spatial resolution of 12″ by 6″ and spectral resolution of 4 km s^{-1} in 1988 and 1990 with the three-element millimeter interferometer at the Hat Creek Radio Observatory. We also remapped the data of the $H^{12}CN$ $J = 1 \rightarrow 0$ spectral line data from Güsten et al. (1987) to match the scale and resolution of our $H^{13}CN$ and HCO^+ maps.

We find that the clumps in the ring have optical depths in $H^{12}CN$ $J = 1 \rightarrow 0$ in the range from 2 to 10 and that the HCO^+ emission is distributed similarly to the HCN emission, but that the abundance ratio $[HCO^+]/[HCN]$ appears to be 5 to 15 times lower than that measured in interstellar, quiescent molecular clouds. Model calculations of the excitation of HCN and comparison with the HCN $J = 3 \rightarrow 2$ intensities, reported by Jackson et al. (1992), suggest that the $[HCN]/[H_2]$ abundance ratio is unusually large. We also find that the diameters of the HCN emission regions in the clumps have diameters ≈ 0.05 to 0.12 pc with molecular gas densities in the range from 0.4 to 5×10^6 cm^{-3}. The most consistent model of the clumps, assuming $T_{gas} \approx 250$ K, has $\tau_{(HCN\ J=1\rightarrow 0)} \approx 4$ and $n(H_2) \approx 2 \times 10^6$ cm^{-3} within regions of diameter $d_{clumps} \approx 0.1$ pc, and molecular abundances $[HCN]/[H_2] \approx 8 \times 10^{-8}$ and $[HCO^+]/[H_2] \approx 10^{-9}$.

Subject headings: Galaxy: center — ISM: molecules — radio lines: ISM

1. INTRODUCTION

In the dynamical center of the Galaxy a circumnuclear rotating ring of cool gas and dust with a radius extending from 1.5 to 7 pc (assuming $R_0 = 8$ kpc) surrounds a cavity of hotter material that may be accreting onto a central massive object. The first indications of the ring came in 1982 when infrared ($\lambda > 50$ μm) observations of dust emission revealed a double-lobed structure, which the authors interpreted as a dust ring of inner radius 1.7 pc centered on the Galactic center with the plane of the ring nearly along the line of sight (Becklin, Gatley, & Werner 1982). Davidson et al. (1992) present more recent dust observations and analyze the heat source requirements. Emission from neutral and low-ionization atoms (O I by Lester et al. 1981; Genzel et al. 1982, 1984; Jackson et al. 1992; H I by Liszt et al. 1983; and C II by Lugten et al. 1986) and from molecules (H_2 by Gatley et al. 1984; CO by Liszt et al. 1983; Harris et al. 1985; Serabyn et al. 1986; Sutton et al. 1990; and HCN by Güsten et al. 1987; Jackson et al. 1992) were also detected from this structure and revealed velocities consistent with a ring rotating at 110 km s^{-1}. A high-resolution image of emission from HCN, obtained by Güsten et al. (1987), delineated an almost complete rotating ring that is tilted by 20° to 25° with respect to the line of sight and 65° to 70° with respect to the plane of the Galaxy. Interior to the ring are warm atomic gas and ionized atoms that are probably a combination of the inner faces of the ring and material from the ring that is most likely falling into the central gravitational potential.

The observations by Güsten et al. (1987) show that the ring is warped, clumpy, and turbulent. They conclude that the clumps have diameters of 0.2 to 0.5 pc and masses of order 300 $M_\odot$ and that they fill a fraction 0.05 to 0.1 of the volume in the ring. Güsten et al. argued that the ring cannot be in a static equilibrium, since the turbulence, sharp inner edge, and clumps in the neutral ring are all unstable features on time scales of 10^4 to 10^6 years. Furthermore, if the ionized streamers are gas falling from the ring into the center, and the current state is typical, then the lifetime of the ring, before it all collects in the center is of the order of 10^6–10^7 yr. Jackson et al. (1992) observed emission from the $J = 3 \rightarrow 2$ transition of HCN and found comparable brightness temperatures as those seen by Güsten et al. for $J = 1 \rightarrow 0$. These authors suggest that the HCN emission lines are opaque and that the H_2 densities are greater than 10^6 cm^{-3} so that the HCN molecular levels are thermalized. They also decompose the emission into four distinct kinematic structures. Observations of CO emission (Sutton et al. 1990), which traces less dense gas than does the HCN emission, suggest clump diameters of 0.1 to 0.2 pc, assuming that there is one clump per 20″ beam.

We have observed the $J = 1 \rightarrow 0$ transitions of $H^{13}CN$ and HCO^+ in the molecular ring. In our analysis we evaluate opacities, densities, and relative abundances of HCN and HCO^+ in the clumps. The $H^{13}CN$ emission enables us to estimate the optical depths of the $H^{12}CN$. The molecule HCO^+, which is equally as abundant as HCN in typical molecular clouds, requires similar H_2 densities as HCN to be seen in emission in the $J = 1 \rightarrow 0$ transition and therefore should trace the same density gas. However, since its abundance depends on the ionization fraction and the chemical pathways for its production are different from those of HCN, HCO^+ is a useful additional probe of the chemical processes occurring in the molecular ring. Estimates of the physical conditions in the ring from previous studies involve dust temperatures of 60 to 100 K (Becklin et al. 1982; Drapatz et al. 1985; Lester et al. 1987), atomic gas temperatures and densities of 300 K and 10^5 cm^{-3} (Genzel et al. 1985; Lugten et al. 1986), and molecular gas temperatures and densities of 100 to 400 K and 0.2 to 4×10^5 cm^{-3} (Harris et al. 1985; Sutton et al. 1990; Serabyn, Güsten, & Evans 1988; see also Serabyn & Güsten 1986).

As we show in § 4.1, below, we find that the relative abundance of HCO^+ relative to HCN is lower than typically

[1] Astronomy Department, Haverford College, Haverford, PA 19041.
[2] Radio Astronomy Laboratory, University of California, Berkeley, CA 94720.

© American Astronomical Society • Provided by the NASA Astrophysics Data System

1993ApJ...411..667M

measured. In § 4.2 we analyze the excitation of the HCN molecules, using more detailed calculations than those of Güsten et al. (1987) and including the $J = 3 \rightarrow 2$ brightness temperatures obtained by Jackson et al. (1992). Our calculations in § 4.2 suggest that it is the HCN abundance that is atypical. We also find that the HCN emission comes from sub-thermally excited molecules from regions of diameter 0.05 to 0.12 pc and molecular gas density 0.4 to 5×10^6 cm^{-3}.

2. OBSERVATIONS

We observed the $J = 1 \rightarrow 0$ molecular transitions lines of $H^{13}CN$ and HCO^+ at 86.340 and 88.189 GHz, respectively, with the three-element, millimeter interferometer at the Hat Creek Radio Observatory.[3] Observations with the B-array were made in 1988 during the months April to July and with the A-array in 1990 from January to April. A total of 30 baselines with the three 6.1 m antennas were obtained with projected spacings from 4.5 to 195 m. The pointing center was at the position of Sgr A*. The total integration time was 88 hr.

A 512-channel correlator (Urry, Thornton, & Hudson 1985) was used to obtain cross correlation spectra over a total bandpass of 290 MHz with 1.25 MHz (4.2 km s^{-1}) spectral resolution. The HCO^+ and $H^{13}CN$ lines were observed simultaneously by recording both sidebands of the first LO at 87.8 GHz. The sideband separation is better than 30 dB.

System temperatures were measured throughout the observations and were typically between 300 and 800 K. Mars and Uranus were observed for flux calibration, with flux density estimates from a disk model with surface brightnesses given by Ulich (1981). Instrumental phase variations were corrected by observing the point source NRAO 530. The instrumental passband calibration involved on-line calibration of the spectrometer passband and observations of the continuum sources 3C 273 and 3C 84 to calibrate the total passband response of the remaining components.

The visibility data were imaged with natural weighting and a Gaussian taper of 50% at UV spacings greater than 30 kλ, yielding a synthesized beam oriented N-S of size 12″ by 6″. The average of the channels with velocity magnitudes greater than 250 km s^{-1} was used to estimate the continuum emission. The continuum map was subtracted from each channel map to produce line-minus-continuum maps, or "difference maps." The difference maps were then deconvolved using the CLEAN algorithm. The continuum map was subtracted before the nonlinear CLEAN deconvolution to ensure a uniform subtraction of the continuum. The variation of the sidelobe pattern with frequency is below the rms noise, 0.13 Jy beam^{-1} (0.21 K), in the individual channel maps. In maps of the integrated line emission, which were made by summing the individual difference maps above the $+3\ \sigma$ level, the rms noise is approximately 0.01 Jy beam^{-1}. The data of the $H^{12}CN$ $J = 1 \rightarrow 0$ line at 88.632 GHz of Güsten et al. (1987) were remapped to match the scale and resolution of the $H^{13}CN$ and HCO^+ maps.

3. RESULTS

Figure 1 shows an overlay of the HCO^+ and $H^{12}CN$ emission and demonstrates that the HCO^+ emission is distributed similarly to the HCN emission. They are both concentrated in the molecular ring and are clumped at the same locations. We have labeled the brightest clumps A through F in Figure 1 and show their spectra in Figure 2.

[3] The millimeter interferometer at the Hat Creek Radio Observatory is operated by the Berkeley-Illinois-Maryland Association (BIMA) with support from the National Science Foundation.

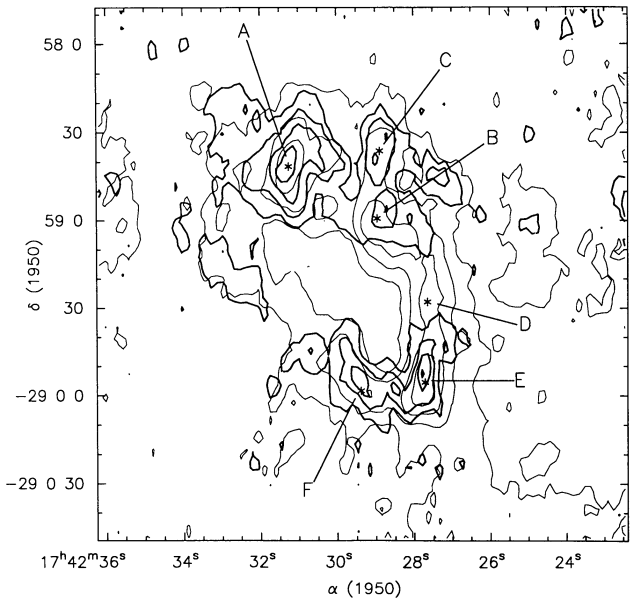

FIG. 1.—Integrated emission from HCO^+ $J = 1 \rightarrow 0$ is shown in thick contours and overlaid with the integrated emission from $H^{12}CN$ $J = 1 \rightarrow 0$, displayed in thin contours. The thick contours correspond to HCO^+ flux-densities of 0.05, 0.10, 0.15, and 0.2 Jy beam^{-1} and the thin contours represent HCN flux-densities of 0.05, 0.15, 0.25, and 0.35 Jy beam^{-1}. The synthesized beams are oriented north-south and have sizes 10.″9 × 5.″5 in the HCO^+ map and 11.″0 × 6.″7 in the HCN map. The labels A through F point to the brightest features, which are discussed in the text. The spectra of features A–E are shown in Fig. 2.

The signal from $H^{13}CN$ is much weaker and close to the noise level over most of the region. However, the brightest $H^{13}CN$ emission peaks do fall on the neutral ring and have spectra with centroids at the same velocity as the $H^{12}CN$ and HCO^+ emission at these positions. We can, then, use the $H^{13}CN$ spectra, which are shown in Figure 2*c*, to determine the $H^{12}CN$ opacities. To ensure that the spectra from all three molecules sample the same area, all channel maps were convolved with a 12″ × 12″ Gaussian before extracting the spectra shown in Figure 2. This 12″ circular beam also allows for direct

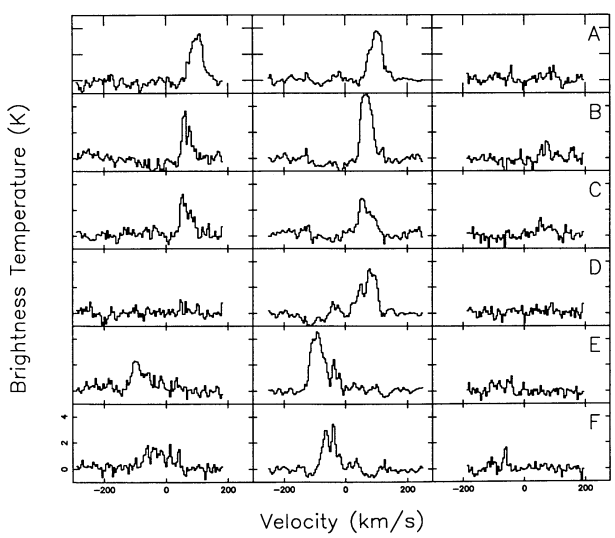

FIG. 2.—Unsmoothed spectra of the emission in (*left*) HCO^+, (*center*) $H^{12}CN$, and (*right*) $H^{13}CN$ at the positions labeled in Fig. 1, convolved with a 12″ × 12″ beam are shown. The spectra are plotted as observed brightness temperature vs. velocity shift relative to the rest frequency of the transition.

© American Astronomical Society • Provided by the NASA Astrophysics Data System

1993ApJ...411..667M

comparison with the HCN $J = 3 \rightarrow 2$ spectra displayed by Jackson et al. (1992).

The HCO^+ emission reproduces the northern and southern ends of the ring, which appears as an ellipse in projection, but is weak along the sides of the ring. As noted by Güsten et al. (1987) the sides of the ring have low Doppler shifts, so the emission is absorbed by line-of-sight clouds. HCO^+ is a stronger absorber in the $J = 1 \rightarrow 0$ transition than is HCN (Carlstrom 1989) and so its absorption is more pronounced. On the other hand, Galactic molecular gas along the line of sight to Sgr A* with velocities above 100 km s^{-1} is rare, so the emission from the ends of the ring, at $|v| \approx 100$ km s^{-1}, travels to the Earth unabsorbed.

Feature D, which is located along the western side of the ring, was noted by Güsten et al. (1987) as having a velocity that is inconsistent with its apparent location in the ring, suggesting that this feature is not part of the ring. We now see that this feature is completely absent in HCO^+. We include feature D in our analysis below, but assume that it is separate from the ring, following Güsten et al. (1987).

4. DISCUSSION

We estimate below the physical conditions in the labeled features using the information provided by the combination of the $H^{12}CN$, $H^{13}CN$, and HCO^+ emission. In § 4.1 we estimate the opacities and relative abundances of $H^{12}CN$ and HCO^+. In § 4.2 we compare the $H^{12}CN$ $J = 1 \rightarrow 0$ brightness temperatures with those at $J = 3 \rightarrow 2$, reported by Jackson et al. (1992), to infer the excitation and conditions of the HCN emission gas.

4.1. *Opacities and Relative Abundances*

We tabulate in Table 1 our estimates of the brightness temperatures and velocities of the peaks of the emission features in the spectra shown in Figure 2. These values are estimated by eye from the general shape of the emission lines. Most of the line profiles are complex and cannot be fit to simple one-component Gaussians. Many of the lines are asymmetric due to the existence of gas at the range of velocities that results in the projection of a tilted rotating ring (Güsten et al. 1987). Additionally, several line profiles contain significant dips due to absorption by previously detected line-of-sight gas (Güsten et al. 1987; Sutton et al. 1990). We account for these absorption dips in our estimation of the peak brightness temperatures by assuming that the intrinsic emission line profiles are obtained by filling in these absorption dips. We do not, however, attempt to estimate the peak values of lines with velocities close to those of the foreground absorption features, which occur at numerous velocities from -70 to $+50$ km s^{-1}. We therefore exclude feature F from Table 1 and from our analysis below.

All of these line-of-sight components, except the -70 km s^{-1} absorption feature seen in our spectra at position E, have been reported in previous studies (cf. Menon & Ciotti 1970; Oort 1977; Scoville 1972; Kaifu, Kato, & Iguchi 1972; Cohen & Few 1976; Liszt & Burton 1978; Beiging et al. 1981; Güsten & Downes 1981). The -70 km s^{-1} feature is present in the Sgr A* H I absorption spectrum of Liszt et al. (1985) and our HCO^+ absorption spectrum (Marr et al. 1992), but is weak and so received no attention. A feature at this velocity is also apparent in emission in CO in the spectra of Sutton et al. (1990). We infer, therefore, that it is a real feature.

To estimate the optical depths of the $H^{12}CN$ emission lines we compare the $H^{12}CN$ and $H^{13}CN$ brightness temperatures. Since the $H^{12}CN$ and $H^{13}CN$ gas should be spatially coincident, we assume that their emission lines have the same beam filling factors and background brightness temperatures. We also assume that they have equal excitation temperatures, which requires that the optical depths not be large enough for line trapping to significantly enhance the $H^{12}CN$ excitation relative to that of the $H^{13}CN$ gas. If line trapping is important, then our optical depth estimates, explained below and given in Table 2, are low. With these assumptions, the $H^{12}CN$ and $H^{13}CN$ optical depths are related by

$$\frac{T_B(H^{13}CN)}{T_B(H^{12}CN)} = \left[\frac{1 - e^{-\tau(H^{13}CN)}}{1 - e^{-\tau(H^{12}CN)}}\right], \quad (1)$$

TABLE 1

EMISSION LINES FROM CLUMPS

Clump (Position) (Relative to Sgr A*)	Central Velocity (km s^{-1})	Line Width (km s^{-1})	Molecule	Peak T_B (K)
A ($-25''.3$, $+36''.5$)	102	50	$H^{12}CN$	3.6
			HCO^+	3.4
			$H^{13}CN$	0.8
			HCN $J = 3 \rightarrow 2$	4.4
B ($+4''.6$, $+18''.9$)	65	60	$H^{12}CN$	4.8
			HCO^+	3.4
			$H^{13}CN$	1.3
C ($+5''.5$, $+41''.7$)	55	60	$H^{12}CN$	2.9
			HCO^+	3.0
			$H^{13}CN$	1.3
			HCN $J = 3 \rightarrow 2$	2.5
D ($+21''.6$, $-9''.4$)	85	75	$H^{12}CN$	3.0
			HCO^+	≤ 1.0
			$H^{13}CN$	0.7
			HCN $J = 3 \rightarrow 2$	2.1
E ($+20''.8$, $-36''.5$)	-96	88	$H^{12}CN$	4.4
			HCO^+	2.2
			$H^{13}CN$	0.7
			HCN $J = 3 \rightarrow 2$	5.0

NOTE.—Uncertainties in the HCO^+, $H^{12}CN$, and $H^{13}CN$ brightness temperatures, given by the rms in the maps, are 0.2 K.

© American Astronomical Society • Provided by the NASA Astrophysics Data System

1993ApJ...411..667M

where T_B is the brightness temperature, defined by $T_B \equiv (\lambda^2/2k)S_\nu$, and where S_ν is the observed flux density. In the limit of small opacities for both species, the right-hand side of equation (1) reduces to the ratio of opacities, which in turn reduces to the ratio of abundances, $Z \equiv [^{12}C]/[^{13}C]$. Previous measurements of Z range from 11 (in Sgr B2, Mangum et al. 1988), and 28 (in the Galactic center, Wannier 1988), to 7 (in the Solar neighborhood, Kaiser, Hawkins, & Wright 1987) and 90 (in the Sun, Lang 1980). Since no $H^{12}CN$ brightness temperature above 5.5 K is found in the data and the detection limit in the $H^{13}CN$ maps is 0.5 K, even with the lowest value of Z emission from $H^{13}CN$ would not be detectable if the $H^{12}CN$ emission were optically thin. Any $H^{13}CN$ emission greater than the noise level, therefore, suggests that the corresponding $H^{12}CN$ emission is optically thick, and that $(1 - e^{-\tau(H^{12}CN)}) \approx 1$. The $H^{12}CN$ brightness temperature, then, is the observed brightness temperature for opaque gas, which we denote by $T_B(thick)$. The $H^{13}CN$ opacity is then

$$\tau(H^{13}CN) \approx -\ln\left[1 - \frac{T_B(H^{13}CN)}{T_B(H^{12}CN)}\right], \quad (2)$$

and the $H^{12}CN$ opacity is

$$\tau(H^{12}CN) = \tau(H^{13}CN)\frac{[H^{12}CN]}{[H^{13}CN]} = \tau(H^{13}CN)Z\ . \quad (3)$$

When the $H^{13}CN$ emission is below detection, we get only an upper limit to $\tau(H^{12}CN)$ by setting $T_B(H^{13}CN) = T_B(noise)$. The $H^{13}CN$ and $H^{12}CN$ opacity estimates are tabulated in Table 2.

Determination of the relative abundances of HCO^+ and $H^{12}CN$ is less certain owing to the possibility of different formation processes. However, as discussed above, the HCO^+ emission appears to come from the same regions as the HCN emission. Therefore, since the HCO^+ $J = 1 \rightarrow 0$ transition has a similar energy level structure as the HCN $J = 1 \rightarrow 0$ transition, we expect that the HCO^+ emission has the same beam filling factor, excitation temperature, and background temperature as the $H^{12}CN$ emission. If so, then the optically thick brightness temperature for HCO^+ is the same as for the HCN, i.e., $T_B(\text{thick, } HCO^+) \approx T_B(\text{thick, } HCN) = T_B(H^{12}CN)$. The optical depth of the HCO^+ emission, then, is given by

$$\tau(HCO^+) = -\ln\left[1 - \frac{T_B(HCO^+)}{T_B(\text{thick})}\right] = -\ln\left[1 - \frac{T_B(HCO^+)}{T_B(H^{12}CN)}\right]. \quad (4)$$

If $\tau(HCO^+) > 5$ then $T_B(HCO^+) \approx T_B(H^{12}CN)$ and we cannot claim to measure the value of $\tau(HCO^+)$ other than to state that if the $H^{12}CN$ emission is opaque then so is the HCO^+ emission. Since the observed HCO^+ and HCN emission lines involve similar energy level structures and assuming that they trace the same gas, the ratio of their optical depths is directly related to the ratio of their abundances by

$$\frac{[HCO^+]}{[HCN]} \approx \frac{\tau(HCO^+)}{\tau(HCN)}\frac{A(HCN)}{A(HCO^+)}, \quad (5)$$

where the A's are the Einstein A-coefficients, which are 2.4×10^{-5} s^{-1} for HCN and 5.5×10^{-5} s^{-1} for HCO^+ (Carlstrom 1989). Therefore, the HCO^+ to HCN abundance ratio is given by

$$\frac{[HCO^+]}{[H^{12}CN]} = 0.44\frac{\tau(HCO^+)}{\tau(H^{12}CN)}. \quad (6)$$

We have estimated the relative abundances of HCO^+ and HCN in the clumps using equations (1)–(6) and summarize our estimates in Table 2.

The previously measured values for Z imply that the inferred values for $[HCO^+]/[HCN]$ in the clumps in the ring are an order of magnitude smaller than typical Galactic values (≈ 1); HCO^+ and HCN are equally common in quiescent, molecular regions with typical Galactic abundances of

$$\frac{[HCO^+]}{[H_2]} \approx \frac{[HCN]}{[H_2]} \approx 10^{-9}$$

(Nyman 1983; Vogel & Welch 1983; Blake et al. 1987). The abundance ratios in clumps A and C are unmeasurable with the current observations, since the brightness temperatures suggest that emission from both molecules is opaque. However, in clumps B and E the HCO^+ brightness temperatures are noticeably smaller than those of $H^{12}CN$, suggesting that the HCO^+ is less abundant than the HCN. The ratio of the abundances, given in column (5) of Table 2, suggest that $[HCO^+]/[HCN]$ in features B and E is on the order of 0.1 for the smallest measured values of Z and as low as 0.06 if Z equals 30, the value measured for the Galactic center by Wannier (1988). We find, then, given the assumptions of equal excitation temperatures and beam filling factors, that the abundance of HCO^+ relative to HCN in the circumnuclear molecular ring is at least an order of magnitude smaller than the typical Galactic value. In clump D, which is probably not part of the ring, we obtain an upper limit to $[HCO^+]/[HCN]$ of 0.07.

The assumptions made here, if wrong, are unlikely to resolve this issue, since allowances for different beam filling factors and different excitation temperatures would have opposing effects.

TABLE 2

OPACITIES

Clump	$\tau(H^{13}CN)$	$\tau(H^{12}CN)$	$\tau(HCO^+)$	$[HCO^+]/[HCN]$
A	0.22 ($\pm$0.06)	0.22 ($\pm$0.06) Z		
B	0.27 ($\pm$0.04)	0.27 ($\pm$0.04) Z	1.2 ($\pm$0.3)	2.0 ($\pm$0.6) Z^{-1}
C	0.45 ($\pm$0.08)	0.45 ($\pm$0.08) Z		
D	0.23 ($\pm$0.07)	0.23 ($\pm$0.07) Z	$\leq$0.41 ($\pm$0.03)	$\leq$0.78 ($\pm$0.24) Z^{-1}
E	0.17 ($\pm$0.05)	0.17 ($\pm$0.05) Z	0.69 ($\pm$0.1)	1.8 ($\pm$0.6) Z^{-1}

NOTES.—$Z = [^{12}C]/[^{13}C]$. The uncertainties are determined from the rms noise in the data and standard propagation of error through eqs. (2), (3), (4), and (6).

© American Astronomical Society • Provided by the NASA Astrophysics Data System

1993ApJ...411..667M

Since the $J = 1 \rightarrow 0$ emission line of HCN has a slightly lower critical density than that of the HCO^+ emission line, the HCN could be in slightly higher density gas and could therefore have a higher excitation temperature. This would make T_B(thick) for the HCN greater than for the HCO^+ and change the inferred $[HCO^+]/[HCN]$ ratio toward a more typical value. However, since the clumps probably have increasing density toward their centers, this would also imply that the HCN is more centrally concentrated in the clumps than the HCO^+ and therefore would have a smaller beam filling factor, thereby lowering T_B(thick) for the HCN relative to that for the HCO^+. On the other hand, the lower brightness temperatures for HCO^+ could be indicating that the HCO^+ and HCN are not similarly distributed but that the HCO^+ is actually more centrally concentrated in the clumps. Its emission, in this case, would have a smaller beam filling factor and therefore a smaller T_B(thick). However, this then requires an explanation for why $[HCO^+]/[HCN]$ is so low in abundance in the lower density molecular gas and so high in the high-density gas. The assumptions of equal excitation temperatures and beam filling factors, then, corresponds to the least contrived situation.

Even though a large flux of ionizing radiation exists in Sgr A West, as evidenced by the ionized gas streamers, we need not expect an enhanced abundance of HCO^+ due to a high ionization fraction in the molecular ring. The regions probed in this study, with H_2 densities greater than 10^5 cm^{-3}, are at the centers of high optical depth clumps and therefore are shielded from external radiation sources. Additionally, Serabyn & Lacy (1985) point out that the neutral ring appears to be shielded from the central radiation by the ionized gas streamers. However, our data suggest values of $[HCO^+]/[HCN]$ that are lower than typical. Some possible mechanisms responsible for a low $[HCO^+]/[HCN]$ include the following:

1. The large column depths of the clumps provide shielding from cosmic ray ionization and so may lead to lower fractional ionization than in typical Galactic clouds and hence lower abundances of HCO^+ (Watson 1974; Vogel et al. 1984; Fukui et al. 1980; Blake et al. 1987).

2. At the temperatures modeled to exist in the neutral ring, $T \approx 250$ K, complete evaporation of grain mantles should occur, which can lead to an enhancement of HCN (Tielens & Hagen 1982; Blake et al. 1987). Observations of HDO in the neutral ring will help to determine if there is grain evaporation (Moore, Langer, & Huguenin 1986; Plambeck & Wright 1987) and possibly to what extent it occurs to affect the value of $[HCO^+]/[HCN]$. Since HDO is destroyed by gas phase reactions, its detection would also yield information about timescale estimates of the grain evaporation.

3. The shocks that probably occur in the ring (Güsten et al. 1987; Gatley et al. 1984) should have significant effects on the HCO^+ and HCN abundances. However, the exact effect of shocks on the chemical dynamics is in dispute. Blake et al. (1987) and Mitchell & Deveau (1983) have argued that the abundance of HCN may be enhanced in hot, shocked regions, while others have argued that high-velocity shocks enhance HCO^+ abundances (e.g., Vogel et al. 1984).

4.2. *Physical Conditions*

Jackson et al. (1992) show spectra of the HCN $J = 3 \rightarrow 2$ emission lines at various points in the ring, four of which coincide with our features A, C, D, and E. We have included in Table 1 the HCN $J = 3 \rightarrow 2$ brightness temperatures estimated from the spectra shown by Jackson et al. (1992). In the features known to be in the ring, A, C, and E, the brightness temperatures of the $J = 3 \rightarrow 2$ transition are all greater than 0.85 of those that we see in $J = 1 \rightarrow 0$. Considering the noise level in the data, the brightness temperatures could actually be equal, as would be the case for completely thermalized molecules. We have obtained estimates of the lower limits to the molecular gas density in the clumps in the ring by requiring that the observed $J = 3 \rightarrow 2$ brightness temperatures be at least 0.9 of those in $J = 1 \rightarrow 0$. We have modeled the statistical equilibrium excitation of HCN using a program developed by W. T. Reach, B.-C. Koo, & W. J. Welch (1989, private communication) that involves calculations similar to those described by Goldreich & Kwan (1974). The calculations predict the excitation temperatures, brightness temperatures, and opacities for the first 20 levels for given values of gas temperature, density, and $\tau(J = 1 \rightarrow 0)$. The effects of dust and line-trapping were included and no external photoexcitation source, other than the 2.7 K background, was assumed. We inferred from Becklin et al. (1982) and assumed for our calculations a dust temperature of 75 K and intensity at 100 μm of 2×10^5 MJy s^{-1} in the regions of the clumps. We constrained the range of parameter space of the input values by limiting the gas temperature to be between 150 and 450 K, as suggested by previous studies, and the optical depths of the $J = 1 \rightarrow 0$ emission line to be between 1 and 12, as suggested by Table 1 with the assumption that Z is between 10 and 40 in the Galactic center region. We have also inferred upper limits to the molecular gas densities by requiring that the HCN $J = 1 \rightarrow 0$ emission line not be a maser. We list in Table 3 the range of allowed conditions, assuming that the gas temperatures are in the range inferred in previous studies of the ring, i.e., 150 to 450 K.

The sizes of the clumps, $d_{\rm clump}$, can also be inferred from the beam filling factors and beam size. The beam filling factor, $f_{\rm bm}$, given by the ratio of the observed brightness temperature to the modeled brightness temperature, relates to the angular

TABLE 3

ALLOWED CONDITIONS IN HCN EXCITATION MODEL

$T_{\rm gas}$ (K)	$\tau(J = 1 \rightarrow 0)$	$n(H_2)$ ($\times 10^6$ cm^{-3})	f_0	$T_{\rm ex}$ (K)	T_B (K)	d(clump) (pc)	$[HCN]/[H_2]$
150	1	min: 4	0.094	62.2	35.1	0.12	6×10^{-9}
		max: 5	0.084	70.2	40.2	0.12	6×10^{-9}
150	12	min: 0.8	0.069	67.2	60.6	0.09	6×10^{-7}
		max: 5	0.038	113.6	106.9	0.07	4×10^{-7}
450	1	min: 2.5	0.088	66.7	38.0	0.12	1×10^{-8}
		max: 3	0.074	79.9	46.3	0.11	1×10^{-8}
450	12	min: 0.4	0.067	67.4	60.8	0.09	1×10^{-6}
		max: 3	0.021	195.9	189.3	0.05	3×10^{-6}

© American Astronomical Society • Provided by the NASA Astrophysics Data System

1993ApJ...411..667M

diameter of a clump, θ, by $f_{bm} \approx \pi(\theta/2)^2$/beam area. For $R_0 = 8$ kpc, then, the clump diameter in pc is given in our study by

$$d = 0.33\left[\frac{T_B(\text{observed})}{T_B(\text{modeled})}\right]^{1/2}.$$

Assuming a gas temperature of 250 K, which is most consistent with all previous studies of the ring, and $Z = 20$, our calculations show that a density of 2×10^6 cm^{-3} fits the observed brightness temperatures best, yielding $T_{ex} \approx 70$ K and $d_{clump} \approx 0.1$ pc. In a study of emission from CO in the neutral ring. Sutton et al. (1990) infer densities in the range 0.2 to 2×10^5 cm^{-3} and beam filling factors that imply clump diameters of 0.1 to 0.2 pc. Since HCN requires higher densities to be seen in emission than does CO, our observations probe deeper into the clumps and hence to higher densities than do those of Sutton et al. Therefore, our results are consistent with those of Sutton et al. and, in combination, provide estimates of the molecular gas density at two different radii of the clumps.

Also listed in Table 3 are the abundances of HCN relative to H_2 for the allowed conditions. We infer the HCN to H_2 abundance ratio from the ratio of their column depths. The column depth of HCN emission is given by

$$N(\text{HCN}) = 3 \times 10^6 \frac{\tau \Delta v}{(f_0/g_0)[1 - \exp(-4.26/T_{ex})]}$$

(Marr 1990), where Δv is the width of the line in Hz, τ is the optical depth, f_0 is the fraction of HCN molecules in the ground state, g_0 is the statistical weight of the ground state, and T_{ex} is the excitation temperature of the $J = 1 \rightarrow 0$ transition. In the emission lines we observed, $\Delta v = 40$ km s^{-1} $= 1.7 \times 10^7$ Hz, and f_0 is calculated in our model and listed in Table 3. The column depth of H_2 is simply $N(H_2) = n(H_2) \times d$, where d is the diameter of a clump in cm. The abundance of HCN relative to H_2, then, is

$$\frac{[\text{HCN}]}{[\text{H}_2]} = 5.1 \times 10^{13} \frac{\tau}{n(\text{H}_2) df_0[1 - \exp(-4.26/T_{ex})]}$$

Note that the lowest allowed value of $[HCN]/[H_2]$ in Table 2 is 6×10^{-9}, and that occurs only for the lowest value of the gas temperature and $\tau = 1$, which requires a value of Z of only 4 to 7. With more reasonable numbers, e.g., $\tau(J = 1 \rightarrow 0) = 4$, $T = 250$ K, and $n(H_2) = 2 \times 10^6$ cm^{-3} we get $[HCN]/[H_2] \approx 8 \times 10^{-8}$. Typical interstellar abundances of HCN are $\approx 10^{-9}$. Therefore, we infer that the HCN relative abundance is more than an order of magnitude greater than typical in molecular clouds.

5. CONCLUSIONS

The following conclusions can be inferred from the observations presented in this paper:

1. The $H^{12}CN$ emission is opaque in the clumps, as suggested by the strong $H^{13}CN$ emission, and the emitting HCO^+ and HCN molecules are very similarly distributed in the 2 pc molecular ring.

2. Our data suggest that the abundance of HCO^+ in the ring is 0.06 to 0.2 of the HCN abundance, whereas these molecules are equally abundant in quiescent molecular clouds. Model calculations of the HCN excitation fitted to the observed brightness temperatures in $J = 1 \rightarrow 0$ and $J = 3 \rightarrow 2$ suggest that it is the HCN that has an atypical abundance. Enhancement of HCN could result from grain evaporation at the high temperatures in the clumps, while a depletion of HCO^+ could result because of shielding from cosmic rays. Shocks might also be important in affecting the $[HCO^+]/[HCN]$ ratio and need further study.

3. The ratio of the $J = 1 \rightarrow 0$ and the $J = 3 \rightarrow 2$ brightness temperatures suggest that the clumps of HCN emission are 0.05 to 0.12 pc with $n(H_2) = 0.4$ to 5×10^6 cm^{-3}. The best-fit model involves clump diameters of ~ 0.1 pc and $n(H_2) \sim 10^6$ cm^{-3} and $[HCO^+]/[HCN] \sim 8 \times 10^{-8}$.

We are grateful to Bill Reach for providing the modeling program, to Patricia Carral for helpful discussions, and to Fronefield Crawford for assistance in the data analysis.

Partial support for this research was provided by NSF grants AST-8714721, AST-910306, AST-8815528, AST-9003404, and AST-8914988.

REFERENCES

Becklin, E. E., Gatley, I., & Werner, M. W. 1982, ApJ, 258, 135
Beiging, J., Downes, D., Wilson, T. L., Martin, A. H. M., & Güsten, R. 1981, A&A, 42, 163
Blake, G. A., Sutton, E. C., Masson, C. R., & Phillips, T. G. 1987, ApJ, 315, 621
Carlstrom, J. E. 1989, Ph.D. thesis, Univ. California-Berkeley
Cohen, R. F., & Few, R. W. 1976, MNRAS, 176, 495
Davidson, J. A., Werner, M. W., Wu, X., Lester, D. F., Harvey, P. M., Joy, M., & Morris, M. 1992, ApJ, 267, 174
Drapatz, S., Haser, L., Hofmann, R., Oda, N., & Wilczek, R. 1985, Adv. Space Res., 5(3), 7
Fukui, Y., Kaifu, N., Morimoto, M., & Miyaji, T. 1980, ApJ, 241, 147
Gatley, I., Jones, T. J., Hyland, A. R., Beattie, D. H., & Lee, T. J. 1984, MNRAS, 210, 565
Genzel, R., Watson, D. M., Crawford, M. K., & Townes, C. H. 1985, ApJ, 297, 766
Genzel, R., Watson, D. M., Townes, C. H., Lester, D. F., Dinerstein, H., Werner, M., & Storey, J. 1982, in AIP Conf. Proc. No. 83, The Galactic Center, ed. G. R. Riegler & R. D. Blandford (NY: AIP), 72
Genzel, R., Watson, D. M., Townes, C. H., Dinerstein, H. L., & Hollenbach, D. 1984, ApJ, 276, 551
Goldreich, P., & Kwan, J. 1974, ApJ, 189, 441
Güsten, R., & Downes, D. 1981, A&A, 99, 27
Güsten, R., Genzel, R., Wright, M. C. H., Jaffe, D. T., Stutzki, J., & Harris, A. I. 1987, ApJ, 318, 124
Harris, A. I., Jaffe, D. T., Silber, M., & Genzel, R. 1985, ApJ, 294, L93
Jackson, J. M., Geis, N., Genzel, R., Harris, A. I., Madden, S., Poglitsch, A., Stacey, G. J., & Townes, C. H. 1992, preprint
Kaifu, N., Kato, T., & Iguchi, T. 1972, Nature Phys. Sci., 238, 105
Kaiser, M. E., Hawkins, I., & Wright, E. L. 1991, ApJ, 379, 267
Lang, K. R. 1980, Astrophysical Formulae, 2d ed. (NY: Springer)
Lester, D. F., Joy, M., Harvey, P. M., & Ellis, H. B. 1987, in AIP Conf. Proc. No. 155, The Galactic Center, ed. D. C. Backer (NY: AIP), 138
Lester, D. F., Werner, M. W., Storey, I. W. V., Watson, D. M., & Townes, C. H. 1981, ApJ, 248, L109
Liszt, H. S., & Burton, W. B. 1978, ApJ, 226, 790
Liszt, H. S., Burton, W. B., & van der Hulst, J. M. 1985, A&A, 142, 245
Liszt, H. S., van der Hulst, J. M., Burton, W. B., & Ondrechen, M. P. 1983, A&A, 126, 341
Lugten, J. B., Genzel, R., Crawford, M. K., & Townes, C. H. 1986, ApJ, 306, 691
Mangum, J. G., Rood, R. T., Wadiak, E. J., & Wilson, T. J. 1988, ApJ, 334, 182
Marr, J. M. 1990, Ph.D. thesis, Univ. California-Berkeley
Marr, J. M., Pauls, T., Rudolph, A., Wright, M. C. H., & Backer, D. C. 1992, ApJ, 400, L29
Menon, T. K., & Ciotti, J. E. 1970, Nature, 227, 579
Mitchell, G. F., & Deveau, T. J. 1983, ApJ, 266, 646
Moore, E. L., Langer, W. D., & Huguenin, G. R. 1986, ApJ, 306, 682
Nyman, L.-A. 1983, A&A, 120, 307
Oort, J. H. 1977, ARA&A, 15, 295
Plambeck, R. L., & Wright, M. C. H. 1987, ApJ, 317, L101
Scoville, N. Z. 1972, ApJ, 175, L127
Serabyn, E., & Güsten, R. 1986, A&A, 161, 334
Serabyn, E., Güsten, R., & Evans, N. J. 1988, in IAU Symp. 136, The Center of the Galaxy, ed. M. Morris (Dordrecht: Kluwer), 417
Serabyn, E., Güsten, R., Walmsley, C. M., Wink, J. E., & Zylka, R. 1986, A&A, 169, 85

© American Astronomical Society • Provided by the NASA Astrophysics Data System

1993ApJ...411..667M

Serabyn, E., & Lacy, J. H. 1985, ApJ, 293, 445
Sutton, E. C., Danchi, W. C., Jaminet, P. A., & Masson, C. R. 1990, ApJ, 348, 503
Tielens, A. G. G. M., & Hagen, W. 1982, A&A, 114, 245
Ulich, B. L. 1981, AJ, 86, 1619
Urry, W. L., Thornton, D. D., & Hudson, J. A. 1985, PASP, 97, 745
Vogel, S. N., & Welch, W. J. 1983, ApJ, 269, 568
Vogel, S. N., Wright, M. C. H., Plambeck, R. L., & Welch, W. J. 1984, ApJ, 283, 655
Wannier, P. G. 1988, in IAU Symp. 136, The Center of the Galaxy, ed. M. Morris (Dordrecht: Kluwer), 107
Watson, W. D. 1974, in Proc. Les Houches Summer School of Theoretical Physics, Session XXVI, Atomic and Molecular Physics and the Interstellar Matter, ed. R. Balian, P. Encrenaz, & J. Lequeux (Amsterdam: North-Holland), 177

© American Astronomical Society • Provided by the NASA Astrophysics Data System